Journal of Magnetics 7(3), 106-114 (2002)

Control of Thin Film Media Microstructure by Using Very Thin Seedlayer Material with Different Affinity for Oxygen

D. D. Djayaprawira*, Satoru Yoshimura[1] and Migaku Takahashi[1]

Department of Electronic Engineering, Graduate School of Engineering, Tohoku Univ., Japan
[1]New Industry Creation Hatchery Center, Tohoku Univ., Japan

(Received 19 August 2002)

To reduce the grain size and the media noise in a typical CrMo/CoCrPtB longitudinal media, a sputtering process which includes the exposure of oxygen onto the surface of CrW_x (x=0, 25, 50, 75, 100 at.%) and $CrTi_{15}$ seedlayers with the thickness of 0.5 nm have been utilized. The main results are: (1) the media grain size and the media noise are reduced when using CrW_x (x=0, 25, 50 at.%) seedlayers, and not reduced when using $CrTi_{15}$ or CrW_x (x=75, 100 at.%) seedlayers, (2) AES and RHEED results suggest that W seedlayer, which has the highest melting point, forms layer-like film with very small and dense island grain, due to its high free surface energy and low mobility. On the other hand, CrW_{50} and Cr seedlayers, which have lower melting point than W seedlayer, form island film, (3) to effectively reduce the media grain size and improve the media signal to noise ratio, it is essential to utilize a very thin Cr-based seedlayer with high affinity for oxygen and which forms island-like structure, such as CrW_{50} seedlayer.

Key words : thin film media, very thin seedlayer, melting point, island or layer-like structure, AES and RHEED.

1. Introduction

High areal density realized in hard-disk drives has been achieved by significant developments in media, head, position tracking, channel and coding technology. To give adequate bit error rates at a specified areal density, it is necessary to maintain signal to noise ratio (*S/N*). This is made possible by reducing the media noise, increasing the sensitivity of the read-head and using suitable channel and coding scheme. To reduce the media noise in longitudinal magnetic recording system, reduction of grain size and its distribution in the magnetic layer is an indispensable requirement [1, 2]. To this end, several techniques such as: reduction of underlayer thickness [3], addition of boron element to CoCr-based magnetic layer [4, 5] and utilization of seedlayers [6-12] have been proposed.

The objective of this article is to provide fundamental understanding in designing media with small and uniform grain size, to realize low noise media for high recording density. We will focus our discussion on grain size reduction method using very thin seedlayers with the melting point in the range of 1600-3400 °C studied by our group [13-18]. The idea of using such kinds of seedlayers was initiated by a preliminary study, which suggested that a very thin seedlayer with high melting point could be used to suppress the grain growth of the succeeding layer which has lower melting point [19]. The very thin seedlayer is suggested to grow as islands, which work as nucleation sites to suppress the grain growth of the succeeding layer.

This paper is structured as follows: The Introduction is followed by an Experimental section describing the sample preparation and evaluation methods. In Section 3, the effect of very thin high melting point seedlayer on the media properties is discussed. To clarify the mechanism of the grain size reduction using the seedlayer, the initial growth form of the seedlayers with various compositions was examined. We shall show that the seedlayer forms an island like structure in its initial growth process, and the initial growth form is strongly correlated with the melting point of the seedlayer material. Furthermore, we shall show that the microstructure of the media using the seedlayer strongly depend on the initial growth form of the seedlayer. In Section 4, the effect of exposing oxygen onto the seedlayer surface on the media properties is also discussed. The purpose of exposing oxygen onto the

*Corresponding author: D. D. Djayaprawira, Tel: +81-22-217-7134, e-mail: david@ecei.tohoku.ac.jp

seedlayer surface is to enhance the nucleation sites of the seedlayer. We show that the combination of using the seedlayer and oxygen exposure process is most effective to reduce the grain size and the media noise of thin film media. In Section 5, a guiding principle to design low noise media using a very thin seedlayer and oxygen exposure process is presented. Finally, we summarize the results in the Conclusion.

2. Experimental

Thin film media with the structure of (Cr, CrW_{25}, CrW_{50}, CrW_{75}, W, or $CrTi_{15}$) seedlayer (0.5 nm)/ $CrMo_{15}$ underlayer (10 nm)/$CoCr_{24}Pt_{12}B_4$ magnetic layer (20 nm)/ C protective layer (7 nm) were deposited onto non-textured and circumferentially textured NiP/Al disk substrates by DC magnetron sputtering system under the base pressure of about 3×10^{-9} Torr (C3010P7-UHV: Anelva Co., Ltd.). The samples deposited on the non-textured substrate were used for Auger Electron Spectroscope (AES), Reflection High Energy Electron Diffraction (RHEED), X-ray diffraction (XRD) and transmission electron microscopy (TEM) analyses, while those deposited on the textured substrate were used for evaluation of magnetic and recording properties. Prior to deposition, the substrate was preheated at 250 °C. Two kinds of media fabrication processes were studied. In the first one (discussed in section 3), after the seedlayer deposition, a RF dry-etching process using Ar gas was applied to remove the adsorbed gases which may exist on the substrate surface [20]. After dry-etching, the underlayer, the magnetic layer and the protective layer were subsequently deposited. In further discussions, we shall address this fabrication process using the term Process A. In another process (discussed in section 4 and 5), after dry-etching, the seedlayer was exposed to oxygen atmosphere which corresponds to adsorption of oxygen atom from 5 layers to 100 layers (5 to 100 L). The other deposition condition was fixed. In further discussions, we shall address this fabrication process using the term Process B. The schematic pictures of both fabrication procedures are shown in Fig. 1.

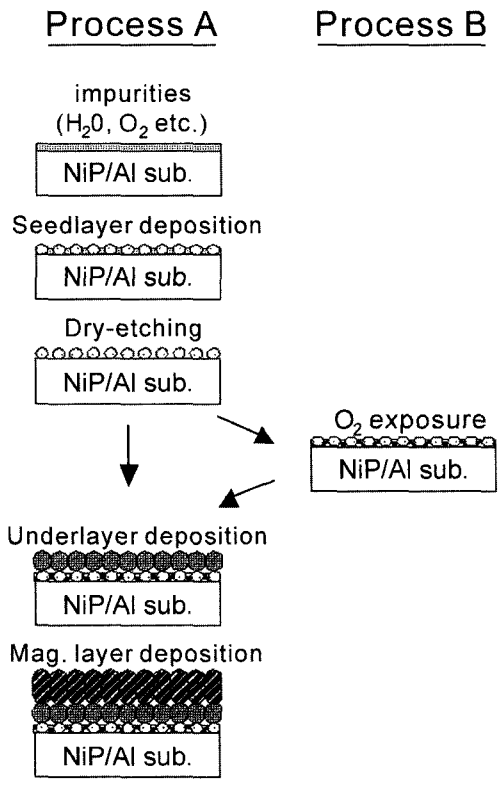

Fig. 1. Schematic pictures of a fabrication procedure in which underlayer was subsequently deposited after seedlayer deposition (Process A), and a fabrication procedure in which the seedlayer was exposed to oxygen atmosphere prior to underlayer deposition.

The growth form of Cr-based seedlayer was examined with an in-situ AES. The schematic top-view diagram of the AES system is shown in Fig. 2. After the seedlayer deposition, the substrate was moved to a sample holder in an analysis chamber using a transfer rod. The sample alignment was controlled using a 5-axes manipulator. The incident angle of the electron beam was about 15°. Due to the low incident angle, high signal to noise ratio of Auger Electron peak can be obtained [21]. The electron acceleration voltage during AES analysis was 4 kV. The crystal-

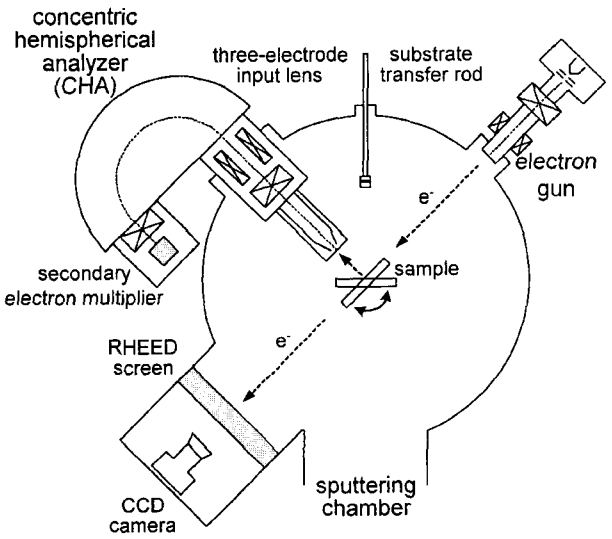

Fig. 2. Schematic top-view diagram of in-situ Auger Electron Spectroscope (AES) and Reflection High Energy Electron Diffraction (RHEED) systems. The analysis systems are attached to a blank chamber of the disk sputtering system.

lographic orientation of the seedlayer was examined in the same analysis chamber with in-situ RHEED analysis. The electron acceleration voltage was 25 keV. The microstructure of the magnetic layer was examined by TEM. The crystallographic orientation of the magnetic layer was analyzed with out-plane XRD ($2\theta/\omega$) and Grazing Incident angle XRD (GID) ($2\theta_\chi/\phi$) methods using Cu-Kα radiation [5]. The magnetic properties were evaluated with a vibrating sample magnetometer (VSM).

3. The effect of very thin high melting point seedlayer on media properties

A. Crystal structure, magnetic and read-write properties of thin film media using very thin high melting point seedlayer

Figure 3 shows the Grazing Incident angle XRD (GID) profiles of the magnetic layer of CoCrPtB media using various seedlayers with the thickness of 0.5 nm fabricated with Process A. For comparison, the GID profile of the media without seedlayer is also shown. The incident angle of the X-ray beam was 0.4°. It is found that hcp(100), hcp(002) and hcp(101) from magnetic layer were the only diffraction peaks observed. In the media without seedlayer and with using Cr, CrW_{25}, CrW_{50}, CrW_{75}, or $CrTi_{15}$ seedlayer, the diffraction peaks intensity is almost the same and shows a fairly high intensity. This

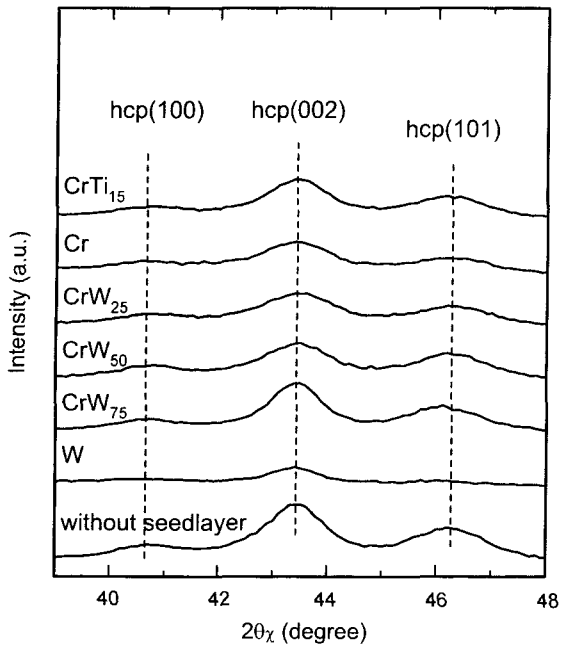

Fig. 3. Grazing incident angle XRD profiles of the magnetic layer of CoCrPtB media using various seedlayers with the thickness of 0.5 nm. The seedlayer compositions are shown in the figure.

Table 1. Magnetic properties of the media with various seedlayers

Seedlayer	H_c (kOe)	S
no-seedlayer	3.5	0.80
$CrTi_{15}$	3.6	0.84
Cr	2.8	0.73
CrW_{25}	3.0	0.76
CrW_{50}	3.5	0.81
CrW_{75}	3.5	0.82
W	2.2	0.56

means that the majority of the c-axes of the magnetic layer in these media are oriented parallel to the substrate plane. On the other hand, in the media using W seedlayer, the diffraction peaks are hardly observed. The result suggests that the c-axes of the magnetic layer of the media are much less oriented to the in-plane direction. From the results we can conclude that except for the media using W seedlayer, introduction of very thin seedlayer does not degrade the in-plane crystallographic orientation of the magnetic layer, which is an important factor to obtain high coercivity and squareness in longitudinal media.

Table 1 shows the magnetic properties of the same media shown in Fig. 3. The table shows that the media without seedlayer and with using Cr, CrW_{25}, CrW_{50}, CrW_{75}, or $CrTi_{15}$ seedlayer show relatively higher coercivity H_c and squareness S. This means that the magnetic properties strongly correlate with the in-plane crystallographic orientation of the media.

In Table 2, reproduced signal S, media noise N, signal to noise ratio S/N and activation grain diameter GD_{act} of media with various seedlayers are shown. Here, S and N were measured at 42 kfci (kilo flux change per inch), and 500 kfci, respectively, while the GD_{act} was determined from the activation volume v_{act} assuming cylindrical shape of the grain. v_{act} was evaluated from the time dependence

Table 2. Reproduced signal S, media noise N, signal to noise ratio S/N and activation grain diameter GD_{act} of the media with various seedlayers. S and N were measured at 42 kfci (kilo flux change per inch), and 500 kfci, respectively

Seedlayer	S (mV_{p-p})	N (mV_{rms})	S/N (dB)	GD_{act} (nm)
no-seedlayer	1.14	0.26	12.8	11.4
$CrTi_{15}$	1.19	0.30	12.0	11.6
Cr	1.00	0.16	16.0	10.7
CrW_{25}	1.06	0.17	15.6	10.6
CrW_{50}	1.14	0.18	15.8	10.7
CrW_{75}	1.19	0.29	12.3	11.4
W	1.01	0.34	9.3	13.1

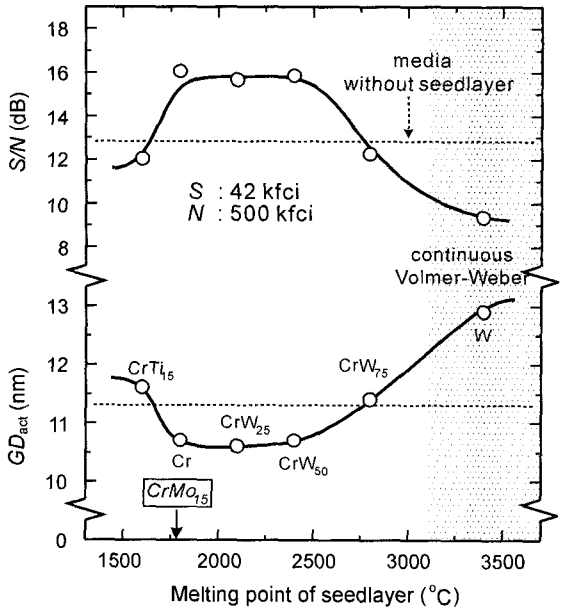

Fig. 4. Media *S/N* and GD_{act} plotted against the melting point MP of the seedlayer.

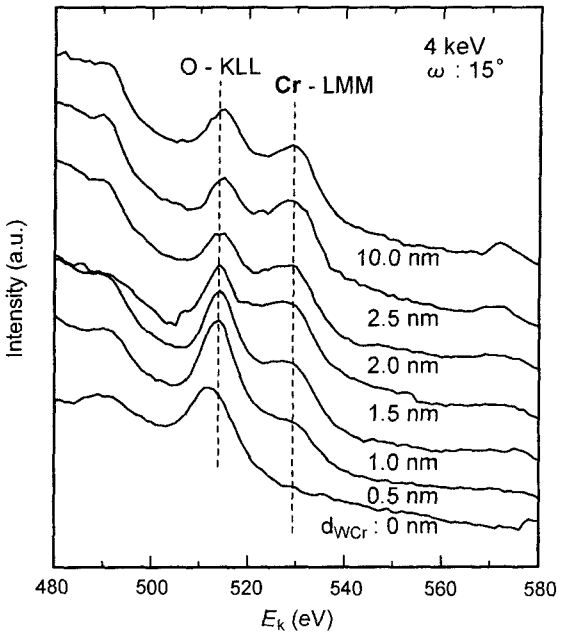

Fig. 5. Typical AES profiles of CrW_{50} seedlayer with various thicknesses.

of remnant coercivity [22]. Here, variation of GD_{act} corresponds to variation of grain size of the magnetic layer [17]. We found that the media *S/N* is increased by 3dB, and GD_{act} is reduced from 11.4 nm to 10.7 nm with using CrW_x (x = 0, 25, 50 at.%) seedlayers. The result shows that CrW_x (x = 0, 25, 50 at.%) seedlayers are effective to reduce the grain size, which results in improvement of media *S/N*.

In Fig. 4, the media *S/N* and GD_{act} are plotted against the melting point MP of the seedlayer [17]. The dash lines show the values of the media without seedlayer. Here, the *MP* of $CrMo_{15}$ underlayer is about 1800 °C. It is found that in the media using the seedlayer with *MP* higher than the $CrMo_{15}$ underlayer, such as Cr, CrW_{25} and CrW_{50}, magnetic grain size is reduced and *S/N* is improved. On the other hand, in the media using the $CrTi_{15}$ seedlayer with *MP* lower than $CrMo_{15}$ underlayer, magnetic grain size GD_{act} is not reduced and *S/N* is not improved. These results are consistent with previous study, which suggested that very-thin seedlayer with high *MP* is effective to reduce the grain size of CrMo/CoCrPtB media [13].

However, GD_{act} is increased and *S/N* is decreased when seedlayer with very high *MP* such as W is used. The results show that utilization of seedlayer with very high melting point is not a sufficient condition to reduce the media grain size. To clarify the mechanism of the variation of the magnetic grain size with the seedlayer, the initial growth form of the seedlayer has been analyzed using AES and RHEED.

B. Analysis of the initial growth form of very thin high melting point seedlayer

Figure 5 shows typical AES profiles of CrW_{50} seedlayer with various thicknesses. An Auger Electron (AE) peak corresponds to Cr (Cr-LMM) was observed at around 530 eV. The AE peak intensity from Cr increases with increasing CrW_{50} seedlayer thickness. Another AE peak at lower kinetic energy region corresponds to oxygen (O-KLL), and was observed independent of the seedlayer thickness. This means that oxygen exists on both the substrate and the CrW_{50} seedlayer. It is suggested that the oxygen on the substrate is a naturally adsorbed one, while the oxygen on the seedlayer is due to oxidation of the seedlayer during observation.

Figure 6 shows the dependence of normalized Auger Electron (AE) peak intensity of W, CrW_{50}, and Cr seedlayers on film thickness. The AE peak intensity is determined by subtracting the AE peak from the background, and is normalized by the AE peak intensity of the film with the thickness of 10 nm. For all seedlayers, with increasing the seedlayer thickness the normalized AE peak intensity increases, which corresponds to the increase of the coverage of the seedlayer on the substrate surface. Saturation of AE peak intensity indicates that the seedlayer has become a continuous film. Taking this into account, the critical thicknesses that W, CrW_{50}, and Cr seedlayers on NiP/Al substrate become continuous films were determined to be 1.5 nm, 2.5 nm, and 5.0 nm, respectively. This result suggests that Cr seedlayer forms

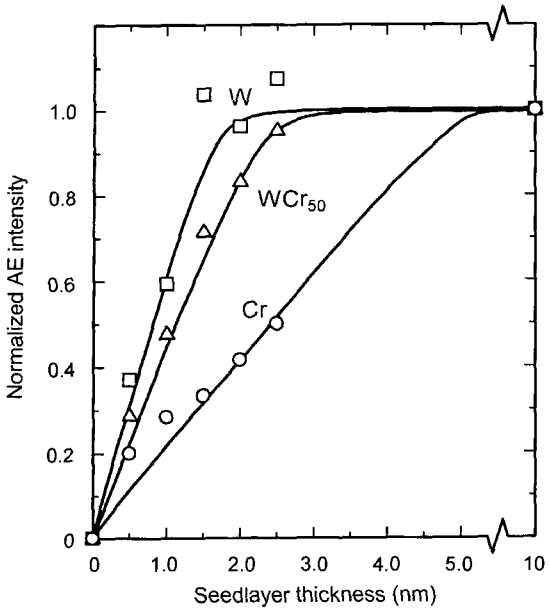

Fig. 6. Dependence of normalized Auger Electron (AE) peak intensity of W, CrW_{50}, and Crseedlayers on film thickness.

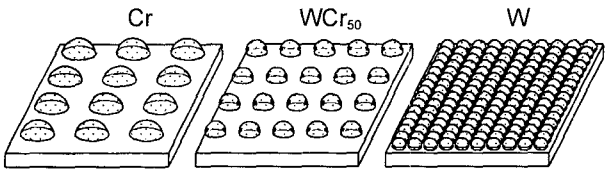

Fig. 7. Schematic models of the initial growth forms of W, CrW_{50}, and Cr seedlayers.

island film, while W seedlayer forms layer-like film. RHEED analysis of W seedlayer with the thickness of 2.0 nm shows ring-like pattern (not shown here). This indicates that the W film is consisted of very small 2D randomly oriented crystal grains.

Considering the above results, schematic models of the initial growth forms of W, CrW_{50}, and Cr seedlayers is shown in Fig. 7. Here, we assume that the growth mode of all the seedlayers is "Volmer-Weber" growth, considering that the seedlayers has melting point considerably higher than the substrate. Taking into account that high melting point material has high surface free energy [23],

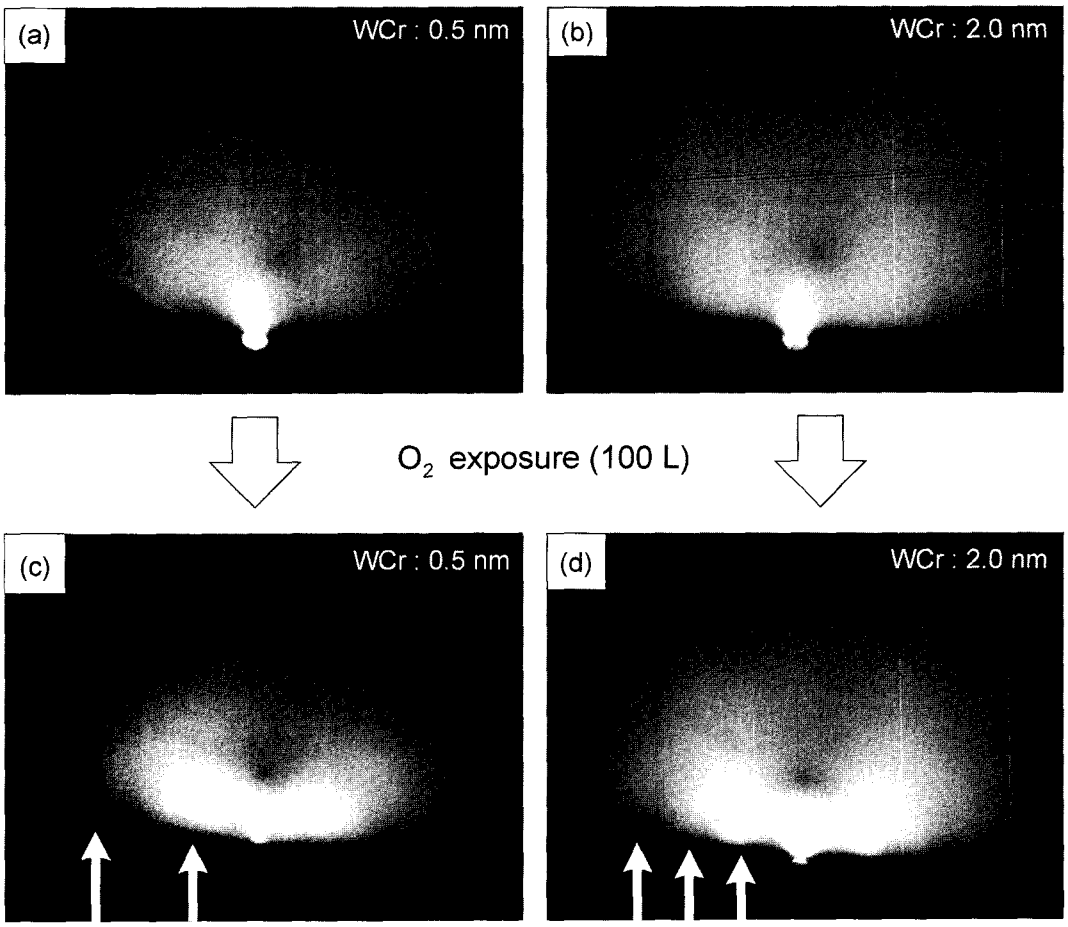

Fig. 8. RHEED images of 0.5 and 2.0 nm WCr_{50} single layer without ((a) and (b)) and with ((c) and (d)) 100 L oxygen exposure.

and that material with high surface free energy has high diffusion energy (low mobility) [24], W seedlayer is suggested to consist of very small and dense island grain which soon cover the substrate surface even when the thickness is very thin. This may explain the reason why W seedlayer forms layer-like film. On the other hand, the Cr or CrW_{50} seedlayer, which has lower melting point compared with W, is thought to form larger and dispersed island grain with lower contact angle relative to the substrate surface.

Finally, the dependence of GD_{act} on the material of the Cr-based seedlayers is explained as following. The fact that GD_{act} is constant in the media using $CrTi_{15}$ seedlayer (*MP* about 1600 °C) is considered to be due to the relatively low surface energy of the seedlayer compared with the $CrMo_{15}$ underlayer (*MP* about 1800 °C). On the other hand, the increase of GD_{act} when using W or CrW_{75}seedlayers is considered to be due to the formation of layer-like film, with very small and dense island grain due to its high free surface energy and low mobility, which reduces the nucleation sites density for the underlayer. The reduction of GD_{act} when using CrW_x (x=0, 25, 50 at.%) seedlayers is suggested to be due to the formation of dispersed island film, and the relatively high surface energy compared with that of the underlayer.

4. The effect of exposing oxygen onto the seedlayer surface on the media properties

A. Crystal structure and grain size

Figure 8 shows the RHEED images of 0.5 and 2.0 nm WCr_{50} single layer without ((a) and (b)) and with ((c) and (d)) 100 L oxygen exposure.fabricated with process B [16]. In the case of CrW_{50} seedlayer without oxygen exposure (Figure 8(a) and 8(b)), RHEED diffraction pattern is not observed. It is thought that these films form an amorphous structure. On the other hand, in the case of the CrW_{50} seedlayer exposed with 100 L oxygen (Figure 8(c) and 8(d)), ring electron diffraction patterns can be observed. The ring width is relatively broad. This implies that these films form a fine crystal grain structure with two-dimensional random orientation. These results show that 100 L of oxygen exposure onto CrW_{50} seedlayer has an effect on enhancing the crystallization of the seedlayer surface.

Figure 9 shows the out of plane XRD patterns of $CrW_{50}/CrMo_{15}/CoCr_{24}Pt_{12}B_4$ media prepared with 0 L (Media A), 25 L (Media B), and 100 L (Media C) of oxygen exposure. The full width at half maximum of diffraction peak rocking curve ($\Delta\theta_{50}$) for CoCrPtB-hcp (110) is also shown. CrMo-bcc(200), CoCrPtB-hcp(110)

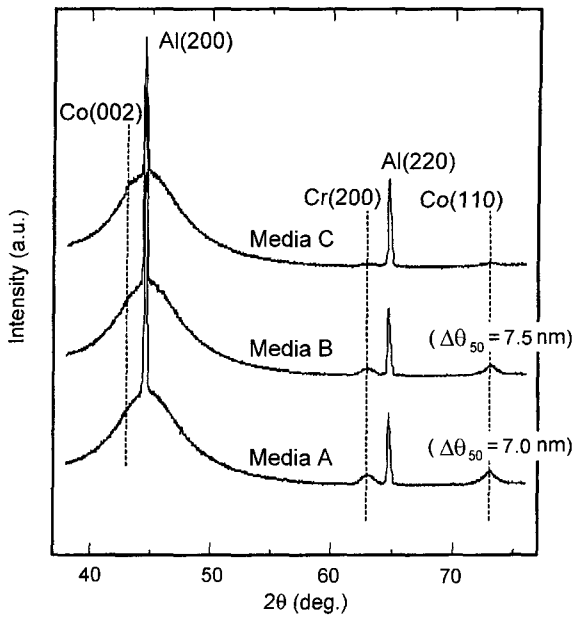

Fig. 9. Out of plane XRD patterns of $CrW_{50}/CrMo_{15}/CoCr_{24}Pt_{12}B_4$ media prepared with 0 L (Media A), 25 L (Media B), and 100 L (Media C) of oxygen exposure.

and diffraction peaks from aluminum substrate were observed in Media A and B. The fact that CoCrPtB-hcp(110) peak of Media A and B shows high intensity means that in-plane orientation of the c-axes of grains of the magnetic layer is realized. The $\Delta\theta_{50}$ of Media A and B is almost constant at 7°. This implies that the crystallographic orientation of the magnetic layer is identical up to 25 L of oxygen exposure. On the other hand, the CoCrPtB-hcp(110) peak for Media C is hardly observed, and it is not possible to measure the $\Delta\theta_{50}$. This indicates that 100 L of oxygen exposure degrades the in-plane orientation of the easy-axes of the magnetic layer. From RHEED analysis it is known that 100 L of oxygen exposure crystallized the seedlayer surface. It is also known that the lattice constant of 20 nm of single layer CrW_{50} film is 3.07 Å with (110) diffraction plane, while the lattice constant of $CrMo_{15}$ film is 2.91 Å with (200) diffraction plane. Therefore, it is thought that the crystallization of seedlayer, the lattice mismatch and the difference of the crystal growth plane between the seedlayer and the underlayer are the main factor for the degradation of longitudinal orientation of the magnetic layer in the media prepared with 100 L of oxygen exposure. Based on this inference, when using this process, choice of a seedlayer which has similar crystal growth plane and lattice constant relative to that of the underlayer, is also important to maintain the c-axes orientation of the magnetic layer.

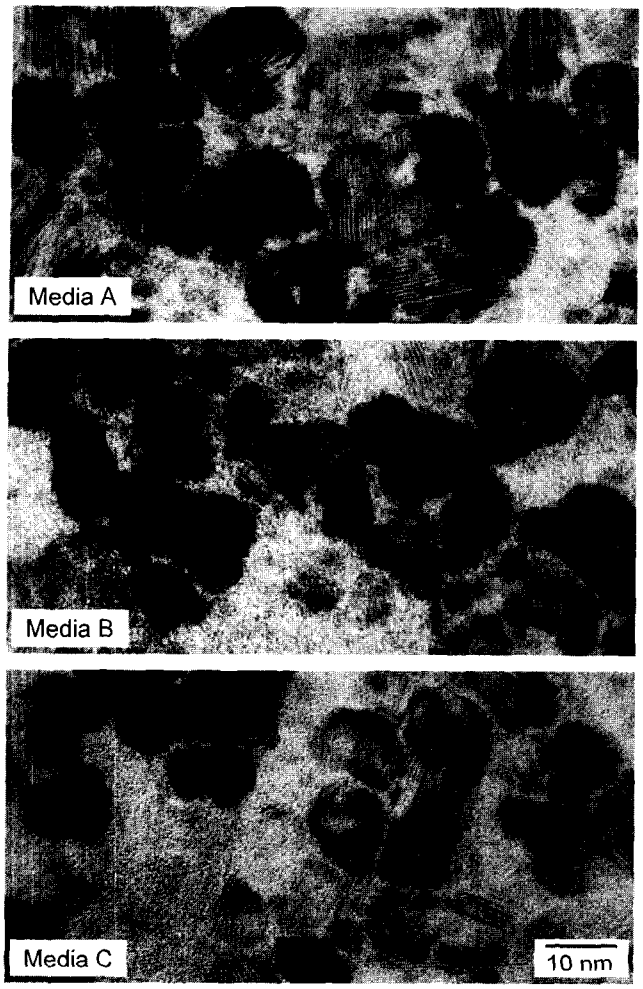

Fig. 10. Plan-view TEM images of $CoCr_{24}Pt_{12}B_4/CrMo_{15}/WCr_{50}$ media prepared with 0 L (Media A), 25 L (Media B), and 100 L (Media C) of oxygen exposure.

Figure 10 shows plan-view TEM images of $CoCr_{24}Pt_{12}B_4/CrMo_{15}/WCr_{50}$ media prepared with 0 L (Media A), 25 L (Media B), and 100 L (Media C) of oxygen exposure. The mean grain size of the magnetic layer was determined by analyzing the TEM images and fitting the distribution of the grain diameter with log-normal function. It is found that mean grain size of Media A, B, and C is 8.3, 7.5, and 7.0 nm, respectively. This result clarifies that the grain size reduces as the amount of the adsorbed oxygen increases, which shows the effectiveness of this process to reduce the grain size. It is thought that the reduction of the grain size is due to enhancement of the nucleation sites of the CrW_{50} seedlayer through partial oxidation.

B. Read-write properties

Figure 11 shows the dependence of reproduced signal output *S*, media noise *N*, signal to noise ratio *S/N*, and recording resolution on the quantity of oxygen exposure.

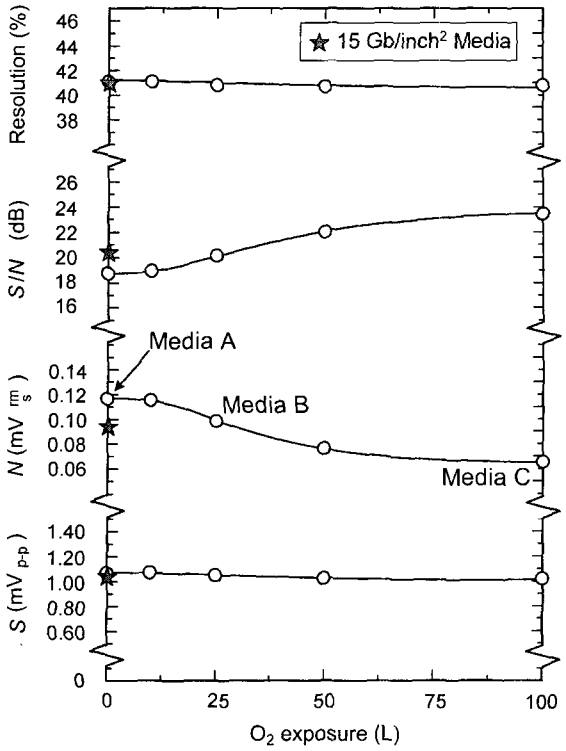

Fig. 11. Dependence of signal output *S*, media noise *N*, signal to noise ratio *S/N*, and recording resolution on the quantity of oxygen exposure.

The recording resolution is the ratio of signal output measured at 250 kfci with *S*. *S* and *N* were measured at 42 and 500 kfci, respectively. For comparison, mass-produced media for 15 Gb/inch^2 disk-drive is also shown. *S* decreases only by 5% with 100 L of oxygen exposure. On the other hand, *N* drastically decreases by 45% with 100 L of oxygen exposure. It is thought that the decrement of *N* is mainly due to the reduction of the grain size as shown in figure 10. As the result, *S/N* significantly increases by 5 dB with 100 L of oxygen exposure. On the other hand, the recording resolution keeps a constant value of about 41%, independent of the quantity of oxygen exposure.

We conclude that this fabrication process is effective to reduce the media noise through grain size reduction while maintaining the recording resolution, which are essential to increase the recording density in longitudinal media.

5. A guiding principle to design low noise media using a very thin seedlayer and oxygen exposure process

Figure 12 shows the dependence of change of activation grain diameter ΔGD_{act} and media signal to noise ratio $\Delta S/N$, when the oxygen exposure quantity was varied from 0

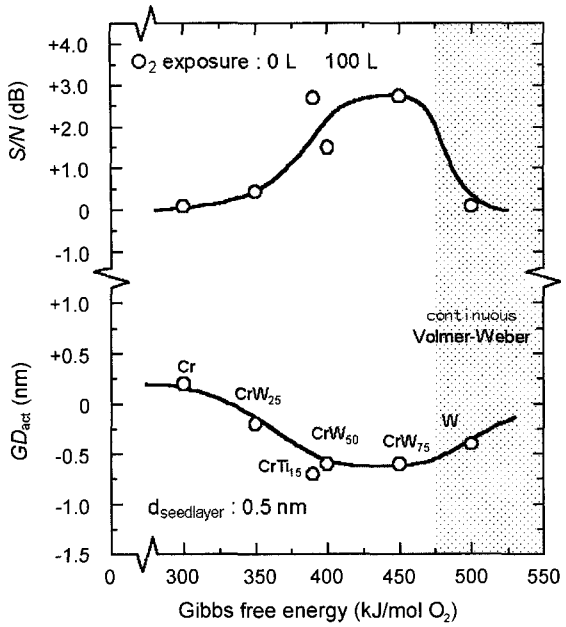

Fig. 12. Dependence of change of activation grain diameter ΔGD_{act} and media signal to noise ratio $\Delta S/N$, when the oxygen exposure quantity was varied from 0 L to 100 L, on standard Gibbs free energy for formation of oxides.

L to 100 L, on standard Gibbs free energy ΔG° for formation of oxides. In the figure, the seedlayer materials are also shown. It is found that with increasing ΔG°, ΔGD_{act} decreases and $\Delta S/N$ increases, except for the media using W seedlayer. From section 4, using Auger Electron Spectroscopy, it is clarified that W seedlayer forms layer-like film, while the other seedlayers form island-like film. The result suggests that to effectively reduce the media grain size and improve the media signal to noise ratio, utilization of very thin Cr-based seedlayer with high affinity for oxygen and which forms island-like structure, such as CrW_{25} or CrW_{50} seedlayer is essential.

6. Conclusion

To reduce the grain size and the media noise in a typical CrMo/CoCrPtB longitudinal media, a sputtering process which includes the exposure of oxygen onto the surface of CrW_x (x=0, 25, 50, 75, 100 at.%) and $CrTi_{15}$ seedlayers with the thickness of 0.5 nm have been utilized. The main results are as follows.

1. The media grain size and the media noise are reduced when using CrW_x (x=0, 25, 50 at.%) seedlayers, and not reduced when using $CrTi_{15}$ or CrW_x (x=75, 100 at.%) seedlayers.

2. AES and RHEED results suggest that W seedlayer, which has the highest melting point, forms layer-like film with very small and dense island grain, due to its high free surface energy and low mobility. On the other hand, CrW_{50} and Cr seedlayers, which have lower melting point than W seedlayer, form island film.

3. To effectively reduce the media grain size and improve the media signal to noise ratio, it is essential to utilize a very thin Cr-based seedlayer with high affinity for oxygen and which forms island-like structure, such as CrW_{50} seedlayer.

References

[1] H. Zhou and H. N. Bertram, *IEEE Trans. Magn.* **35**, 2712 (1999).
[2] M. Takahashi and H. Shoji, *J. Magn. Magn. Mater.* **193**, 44 (1999).
[3] S. Kojima, S. Fukaya, Y. Yahisa, Y. Hosoe, and N. Kodama, *IEEE Trans. Magn.* **31**, 2830 (1995).
[4] Y. Kubota, L. Folks, and E. E. Marinero, *J. Appl. Phys.* **84**, 6202 (1998).
[5] M. Mikami, D. D. Djayaprawira, T. K. Kong, S. Yoshimura, A. Horii, and M. Takahashi, *IEEE Trans. Magn.* **37**, 1484 (2001).
[6] R. Ranjan, J. Chang, T. Yamashita, and T. Chen, *J. Appl. Phys.* **73**, 5542 (1993).
[7] L. L. Lee, D. E. Laughlin, and D. N. Lambeth, *IEEE Trans. Magn.* **30**, 3951 (1994).
[8] L. L. Lee, D. E. Laughlin, and D. N. Lambeth, *IEEE Trans. Magn.* **31**, 2728 (1995).
[9] H. Kataoka, T. Kanbe, H. Kashiwase, E. Fujita, Y. Yahisa, and K. Furusawa, *IEEE Trans. Magn.* **31**, 2734 (1995).
[10] Y. Matsuda, Y. Yahisa, K. Sakamoto, Y. Takahashi, A. Katou, and Y. Hosoe, *IEEE Trans. Magn.* **35**, 2640 (1999).
[11] Zhong-heng Lin, E. T. Yen, J. J. K. Chang, Q. Chen, M. C. Tang, and Ga-Lane Chen, *J. Appl. Phys.* **81**, 3946 (1997).
[12] Y. H. Lee, J. P. Wang, and Li Lu, *J. Appl. Phys.* **87**, 6346 (2000).
[13] S. Yoshimura, D. D. Djayaprawira, H. Shoji, and M. Takahashi, *J. Appl. Phys.* **87**, 6866 (2000).
[14] M. Takahashi, H. Shoji, S. Yoshimura, and D. D. Djayaprawira, *IEEE Trans. Magn.* **36**, 2315 (2000).
[15] S. Yoshimura, D. D. Djayaprawira, A. Horii, M. Mikami, H. Shoji, and M. Takahashi, *J. Magn. Soc. of Japan* **25**, 627 (2001).
[16] S. Yoshimura, D. D. Djayaprawira, M. Mikami, M. Takahashi, K. Komiyama, A. Horii, A. Ohno, and S. Katayama, *J. Appl. Phys.* 2002, in press.
[17] S. Yoshimura, D. D. Djayaprawira, M. Mikami, Y. Takakuwa, and M. Takahashi, *IEEE Trans. Magn.* **38**, 2002, in press.
[18] S. Yoshimura, D. D. Djayaprawira, M. Mikami, M. Taka-

hashi, and Y. Takakuwa, to be published.
[19] M. Tsunoda, T. Ito, M. Takahashi, and T. Shiba, *J. Magn. Soc. Japan* **22**, 457 (1998).
[20] M. Takahashi, A. Kikuchi, and S. Kawakita, *IEEE Trans. Magn.* **33**, 2938 (1997).
[21] F. Shimoshikiryo, "Ph.D. Thesis" (Tohoku University, 1996).
[22] K. Yamanaka, T. Takayama, Y. Ogawa, A. Yano, and T. Okuwaki, *J. Magn. Magn. Mater.* **145**, 255 (1995).
[23] L. Z. Mezey and J. Giber, Jpn. *J. Appl. Phys.* **21**, 1569 (1982).
[24] D. W. Bassett and M. J. Parsley, *J. Phys. D.* 707 (1970).